Research Square

Preprints are preliminary reports that have not undergone peer review.
They should not be considered conclusive, used to inform clinical practice,
or referenced by the media as validated information.

Effect of Drop Height on Ground Deposition Distribution in Helicopter Bucket Firefighting: A Full- Scale Experimental Study

LI Mingxuan[1]

41408990@qq.com

ZHU Xiaobo[2]

Research Article

Keywords: helicopter firefighting, fire bucket, drop height, ground deposition, areal water application, effective coverage area

Posted Date: November 18th, 2026

DOI: https://doi.org/10.21203/rs.3.rs-11538143/v1

License: This work is licensed under a Creative Commons Attribution 4.0 International License.
Read Full License

Additional Declarations: No competing interests reported.

Abstract

Drop height is one of the few operational parameters that pilots can directly control during helicopter bucket drops, yet quantitative field evidence on its influence on ground deposition remains limited. Full-scale drop tests were conducted using an AS350B3 helicopter equipped with a 750 L bucket at heights of 15, 20, and 25 m, with flight speed fixed at 38 kn (approximately 70 km/h). Areal water application was measured gravimetrically using a 51 × 7 sampling grid (357 points). As drop height increased from 15 to 25 m, peak application decreased monotonically from 4.41 to 2.44 L/m² (44.7%), with a larger reduction over 15–20 m (35.8%) than over 20–25 m (13.9%). The deposition centroid shifted 8.5 m downstream, and lateral dispersion increased from 0.78 to 0.95 m. In contrast, longitudinal coverage length (132–141 m) and effective coverage area (1260–1323 m²) varied by less than 7%, indicating that drop height primarily controls deposition intensity and lateral spreading, whereas longitudinal extent is governed mainly by flight speed and release duration. The 20 m case produced the highest mean application over the wetted area (0.93 L/m²), the lowest peak-to-mean ratio (3.06), and the highest recovered-water fraction (41.1%), suggesting the best balance between uniformity and water-use efficiency. Relative to a target coverage range of 0.5–3.0 L/m², operational heights of 15–18 m, approximately 20 m, and 23–25 m are recommended for high-intensity fireline attack, balanced intensity-width objectives, and firebreak/mop-up operations, respectively. Because each condition was tested once, these findings should be validated through replicated trials and fire-behavior experiments.

Introduction

Forest fires are among the most frequent and destructive natural hazards worldwide, characterized by rapid ignition, fast spread, and difficult suppression [1]. In the rugged and highly dissected terrain of southwestern China, complex topography often prevents ground crews from reaching active firelines quickly. Aerial suppression therefore plays a central role because of its rapid response, high mobility, and relative terrain independence [2]. In China, helicopter bucket drops are the most commonly used aerial suppression tactic. Their effectiveness depends jointly on released volume, drop-point accuracy, and the resulting ground deposition pattern [3–4]. Operational practice has produced multiple delivery tactics, including trailing drops in forward flight, hovering release, low-speed release, high-speed swinging drops, and coordinated multi-aircraft drop sequences [5].

The ground deposition pattern of a bucket drop is jointly controlled by drop height, flight speed, wind, and terrain [6]. Most international studies, however, focus on fixed-wing platforms. Amorim [7] developed a numerical model of aerial suppressant delivery that includes column stripping, secondary breakup, and droplet trajectories, and validated it with full-scale tests [8]. Satoh et al. [9] simulated airtanker water release using a two-phase flow framework. Plucinski and Pastor [10] proposed criteria for evaluating aerial suppression performance using drop placement, coverage level, and fire-behavior response, while Giménez et al. [11] reviewed long-term retardant assessment frameworks and application conditions. Although these studies established a foundation for understanding airborne transport and ground deposition, their release conditions differ from helicopter bucket operations, which are typically lower-

speed and more concentrated. Lei et al. [12] recently extended turbulent-jet theory to coordinated multi-aircraft operations and derived analytical optima for release height and aircraft spacing; however, model calibration still requires field measurements of deposition patterns such as those reported here. Plucinski et al. [13] also showed, from 251 wildfire incidents, that aerial suppression reduces containment time mainly when fuels, weather, and topography constrain ground attack.

In China, research on helicopter bucket operations has mainly relied on field observations and operational experience. Wu et al. [3–4] conducted full-scale K-32 tests and reported that 10–20 m drop heights produced more concentrated deposition and improved suppression outcomes, with measurable fire-ground temperature changes caused by drop-point error. Xie et al. [6] used scaled laboratory tests to quantify the effects of inflow velocity and sling length on bucket attitude. Wu et al. [14] simulated H-125 belly-cabin water release and found that lateral spread increased with flight speed, whereas droplet breakup intensified at higher Weber numbers. Despite these advances, quantitative evidence on how drop height affects ground deposition remains limited, particularly for peak intensity, deposit geometry, and effective coverage area. As a result, operational drop height is still selected largely empirically.

To address this gap, this study conducted full-scale bucket-drop experiments using an AS350B3 helicopter with a 750 L bucket at drop heights of 15, 20, and 25 m under constant forward speed. Ground areal application was quantified using gravimetric measurements from a predefined sampling grid. Peak intensity, deposit dimensions, effective coverage area, deposition centroid, and lateral dispersion were then extracted to evaluate how drop height controls deposition structure. Based on these results, preliminary recommendations for operational drop-height selection are proposed.

1. Materials and Methods

1.1 Experimental platform

The tests were carried out at a general aviation base in Guanghan, Sichuan Province, with an AS350B3 helicopter slinging a fire bucket of 750 L rated capacity. The site was flat grassland of uniform vegetation height, about 150 m along the flight direction and 18 m across it — roughly 2 700 m² — with marker flags at the four corners. Tests ran in mid-December under light wind and no precipitation. Air temperature, relative humidity, wind speed and wind direction were logged before each drop, and crosswind speed was held below 3 m/s to keep lateral drift from dominating the deposition pattern. Each drop followed the sequence hover filling – level flight at full load – release at constant height. To fill, the co-pilot pressed the ON button of the bucket control handle to open the valve fully, holding it for at least 3 s, then pressed OFF to close the valve once the level gauge read full. The helicopter climbed to the assigned drop height, flew level along the centreline of the test area at constant speed, and opened the valve once on reaching a pre-marked release line, emptying the bucket in a single pass. Drop height in this paper is the vertical distance from the bottom of the bucket to the ground at the instant of release. The level gauge read full before every drop and the released volume is taken as the bucket's rated capacity.

1.2 Data acquisition system

Measurement points were arranged on a rectangular grid with 51 columns at 3 m spacing along the flight direction and 7 rows at 3 m spacing across it, giving 51 × 7 = 357 points (Fig. 1). At each point, a holder was inserted approximately 10 cm into the soil, and two disposable plastic bowls were placed in the holder ring to collect water. Empty-bowl mass was recorded before each drop; after release, six operators (three teams) weighed all points using electronic balances, and net collected water was obtained by subtraction. Bowl mouth diameter was 17.8 cm (248.8 cm² per bowl), yielding an effective collecting area of 497.6 cm² per point, equivalent to 0.55% of the 3 m × 3 m (9 m²) grid cell represented by each point. Because site width limited the array to seven rows (18 m), lateral metrics (e.g., lateral width and lateral dispersion) are statistically less robust than longitudinal metrics and are used mainly for trend analysis. This 18 m width also defines an upper measurement bound: when non-zero row span reaches 18 m, lateral deposition extends beyond the array, and corresponding lateral parameters, effective coverage area, and recovery ratio should be interpreted as lower bounds.

1.3 Test cases

Drop height was the only experimental variable, while flight speed was kept constant; three cases were defined (Table 1). Case 1 served as the baseline, and Cases 2 and 3 differed only in the vertical distance from bucket bottom to ground, with all other conditions unchanged. Each case included one full-bucket release.

Table 1
Test cases

Case No.	Flight speed/(km/h)	Drop height/m	Note
1	70	15	Baseline case
2	70	20	Drop height changed only
3	70	25	Drop height changed only

Drop height is the vertical distance from the bottom of the bucket to the ground at the instant of release.

1.4 Data processing and parameter definitions

Dividing the net water collected at a point by the effective collecting area of that point gives the unit-area application amount w (L/m²):

$$w = m/(1000\, n_b\, A_b) \quad (1)$$

where m is the net water collected at a point (g), n_b is the number of bowls per point (2), and A_b is the mouth area of one bowl (m²). The unit-area application amount is numerically equivalent to application depth (mm) and corresponds to the internationally used coverage-level metric [10].

Because each point represents a cell area of $A_c = 9$ m², summing the collected water over all points yields the recovered volume within the array, V_Σ, and, relative to the bucket rated capacity Q, the recovery ratio η:

$$V\Sigma = Ac\ \Sigma mi/(1000\ nb\ Ab) \quad (2)$$

$$\eta = V\Sigma/Q \times 100\% \quad (3)$$

where Σm_i is the sum of net water collected at all measurement points in the array (g), and Q = 750 L. The recovery ratio represents the fraction of released water falling within the sampling array and allows cross-case comparison of water-use efficiency.

The spatial distribution of unit-area application amount is represented by a 51 × 7 matrix. Measurement noise below 0.01 L/m² was removed before parameter extraction. This threshold is approximately 1/400 of the peak magnitude: peak intensity and deposition centroid are insensitive to it, whereas effective coverage ratio and effective area, both count-based metrics, are more sensitive. Derived quantities in Table 2 (peak-to-mean ratio, derived recovered volume, and recovery ratio) were calculated from unrounded individual weighings and may differ in the last digit from values back-calculated from rounded table entries.

(1) Peak unit-area application amount w_{max}, the largest value in the distribution matrix, which represents the maximum deposition intensity at a point;

(2) Mean application amount over the non-zero area $\bar{w}$, the arithmetic mean over all non-zero points, which represents the average wetting level of the wetted area;

(3) Longitudinal length L_d and lateral width W_d of the deposit, the ground distances corresponding to the span of non-zero columns and rows, respectively (m);

(4) Effective coverage area S, the number of non-zero points multiplied by the area represented by one point (9 m²), in m²;

(5) Deposition centroid C and dispersion σ, which describe the position and the spread of the bulk of the deposit (m).

The centroid and the dispersion follow from Eqs. (4) and (5):

$$C = \Sigma wi\ xi/\Sigma wi \quad (4)$$

$$\sigma = [\Sigma wi(xi - C)^2/\Sigma wi]1/2 \quad (5)$$

where x_i and w_i are the coordinate (m) and the unit-area application amount (L/m²) of the i-th non-zero point, and the sums run over all non-zero points. Substituting column coordinates gives the longitudinal (column) centroid and dispersion; substituting row coordinates gives the lateral (row) ones.

2. Results and Analysis

2.1 Overall characteristics of deposition patterns

Figure 2 presents the spatial distribution of unit-area application at the three drop heights, and Table 2 lists the corresponding characteristic parameters.

Table 2
Characteristic parameters of deposition distribution at different drop heights

Parameter	15 m	20 m	25 m
Peak unit-area application amount/(L/m²)	4.41	2.83	2.44
Location of peak/(row, column)	(5, 16)	(4, 23)	(5, 19)
Number of non-zero measurement points	147	143	140
Effective coverage ratio/%	41.2	40.1	39.2
Mean application amount over non-zero area/(L/m²)	0.88	0.93	0.67
Peak-to-mean ratio	5.03	3.06	3.65
Total water collected at measurement points/g	1 401.4	1 704.8	1 204.1
Derived recovered volume/L	253.5	308.3	217.8
Recovery ratio/%	33.8	41.1	29.0
Longitudinal deposit length/m	141	132	132
Lateral deposit width/m	15	12	18
Effective coverage area/m²	1 323	1 287	1 260
Longitudinal deposition centroid/m	64.1	71.6	72.6
Lateral deposition centroid/m	11.7	11.1	10.5
Lateral (row) dispersion/m	0.78	0.84	0.95
Longitudinal (column) dispersion/m	8.89	9.50	7.97

The derived recovered volume and recovery ratio follow from Eqs. (2) and (3); all derived quantities come from unrounded individual weighings. Lateral deposit width is the largest span of rows containing non-zero points and is sensitive to isolated points at the edge; at 25 m this value reaches 18 m, the full width of the array, making it a censored value truncated at the boundary, so for that case the lateral parameters, effective coverage area and recovery ratio are lower bounds. The water balance check has not been completed (Section 3.4), so recovery ratios serve only for relative comparison between cases.

Figure 2 and Table 2 show that, at all three heights, deposition forms a strip elongated along the flight direction and narrow in the lateral direction, with most water concentrated within 6–15 m laterally. Along the flight path, deposition is continuous but undulating and multi-peaked, rather than dominated by a single concentrated impact point. This morphology results from column stripping, secondary breakup, and splash at ground impact; the governing mechanisms are discussed in Section 3.2.

As drop height rises from 15 m to 25 m the deposition pattern changes systematically:

(1) Peak deposition intensity decays monotonically. The peak unit-area application amount falls from 4.41 to 2.44 L/m², a reduction of 44.7%, split as 35.8% over 15–20 m and 13.9% over 20–25 m: the rate of decay slows as height increases. The peak-to-mean ratio falls from 5.03 to 3.06 (20 m) and 3.65 (25 m), the lowest value occurring at 20 m, which marks the shift from a highly concentrated deposit to a comparatively uniform one.

(2) Effective coverage area narrows slightly. Non-zero points fall from 147 to 140, the effective coverage ratio from 41.2% to 39.2% and the effective coverage area from 1 323 to 1 260 m² — all by 4.8%, far less than the fall in peak intensity. Raising the height therefore flattens the peak rather than shrinking the area covered.

(3) Recovery ratio inside the array first rises and then falls: 33.8%, 41.1% and 29.0% at 15, 20 and 25 m. At 25 m the measured lateral width reaches the full 18 m of the array, so a substantial share of the water fell outside the array and went uncounted; the value is a lower bound and the true gap between 20 m and 25 m may be smaller than it appears. Section 3.2 examines the causes.

Lateral deposit width varies non-monotonically, at 15, 12 and 18 m, because it is taken as the largest span of non-zero rows and is sensitive to isolated points at the edge. Lateral dispersion, by contrast, increases monotonically from 0.78 to 0.95 m and tracks lateral spreading more reliably, so dispersion is used below as the primary measure of lateral spread. Both the lateral width and the dispersion at 25 m are lower bounds truncated by the array edge; censoring depresses but does not reverse the trend of stronger lateral spreading with height, so the qualitative finding stands, while the increase of 21.8% should be read as a lower limit.

2.2 Deposition profiles along and across the flight direction

Averaging the deposition sideways along and across the flight direction gives the longitudinal and lateral profiles of Fig. 3.

Figure 3(a) shows pronounced multi-peak undulation along the longitudinal profile. At 15 m a steep spike appears near the main peak, with a profile peak of 1.20 L/m² and a high-value segment (above 50% of the profile peak) spanning about 33 m. The curve flattens with height: the profile peak falls to 0.83 L/m² at 20 m and 0.76 L/m² at 25 m, while the high-value segment widens to about 78 m. A lower peak and a broader high-value segment occur together, which means that a greater drop height reduces the extreme non-uniformity of deposition along the flight line.

Figure 3(b) shows a single-peaked lateral profile, peaking 9–12 m across and falling away to both sides. The 15 m case gives the highest lateral peak (1.17 L/m²) on a steep curve; the 20 m case falls slightly to 1.05 L/m² with a similar shape; at 25 m the peak drops to 0.64 L/m² and the curve broadens markedly, indicating more complete lateral spreading. The lateral profile peak differs by only about 10% between the 15 m and 20 m cases, whereas the single-point peak falls by 36% over the same interval, which shows that raising the height to 20 m removes mainly local extremes rather than the laterally averaged amount — consistent with the uniformity assessment drawn from the peak-to-mean ratio in Section 2.1.

2.3 Deposit dimensions and effective coverage area

Figure 4 shows how the peak unit-area application amount, the mean over the non-zero area, the effective coverage area and the number of non-zero points vary with drop height.

Figure 4(a) shows the peak unit-area application amount decaying monotonically with height at a falling rate: peak intensity is most sensitive to drop height in the lower part of the range, and above 20 m further height brings diminishing reduction of the peak.

Figure 4(b) shows the mean over the non-zero area to be essentially flat between 15 and 20 m, rising from 0.88 to 0.93 L/m² (5.7%), then falling at 25 m to 0.67 L/m², a drop of 27.9% from the 20 m value. Peak intensity falls continuously while the non-zero-area mean rises rather than falls at 20 m, which indicates the closest match between wetted area and average wetting level at that height.

Figure 4(c) and (d) show the effective coverage area and the number of non-zero points declining only slightly with height, both by 4.8%, the former staying within 1 260–1 323 m². Longitudinal deposit length varies between 132 and 141 m, a spread of 6.4%; the 20 m and 25 m cases are identical and only the 15 m case is longer, by about 9 m, or three sampling intervals. Back-calculating from $L_d \approx vT$ gives release durations of 7.2, 6.7 and 6.7 s, differing by less than 7% and of the same order as the gravity drain time of a 750 L bucket with the valve fully open; the release duration is therefore treated as equal across cases. On that basis the longitudinal deposit length approximates the product of release duration and flight speed and is barely affected by drop height, so longitudinal extent should be adjusted through flight speed and release timing rather than through height. The back-calculation makes no allowance for longitudinal dispersion during descent or for splash on impact, and therefore gives an upper estimate of the release duration that needs independent verification against valve timing records or high-speed imagery.

2.4 Deposition centroid and dispersion

Figure 5 shows how the deposition centroid and the dispersion vary with drop height.

Figure 5(a) shows the deposition centroid advancing steadily along the flight direction as drop height increases: the longitudinal centroid moves from 64.1 m at 15 m to 71.6 m at 20 m and 72.6 m at 25 m, a total of 8.5 m, of which 7.5 m occurs over 15–20 m and only 1.0 m over 20–25 m — a non-linear pattern,

fast at first and slower afterwards. The lateral centroid moves from 11.7 m to 10.5 m, a shift of only 1.2 m, so drop height has little influence on the lateral position of the deposit.

The forward shift can be checked against the horizontal displacement travelled during descent. Let T be the release duration and τ the effective fall time after allowance for aerodynamic dissipation. If the rate of release is uniform along the path, the centroid measured from the point of release satisfies $C \approx vT/2 + v\tau$; with T the same in every case (Section 2.3), the difference in centroid between two cases equals $v\Delta\tau$. At a flight speed of 19.6 m/s (38 kn), water in free fall from 15 m and 25 m takes 1.75 s and 2.26 s respectively, giving horizontal displacements of 34.2 m and 44.1 m and a difference of 9.9 m; the measured shift is 8.5 m, a relative deviation of about 14%. That the measured value is the smaller of the two agrees with drag dissipating the horizontal momentum of the droplets and making the actual displacement less than the free-fall estimate. Limited by the 3 m sampling interval — a time resolution of 0.15 s — and by unquantified random deviations from bucket swing and rotor downwash, the result is an order-of-magnitude check only, and is offered as a field rule of thumb: each additional 10 m of drop height moves the deposit about 8–10 m forward along the flight line.

Figure 5(b) shows lateral dispersion increasing monotonically with height, from 0.78 to 0.95 m, running opposite to the trend in peak intensity and reflecting the link between greater height, stronger lateral spreading and lower peak intensity. Longitudinal dispersion fluctuates within 8.0–9.5 m, consistent with the longitudinal distribution being governed mainly by flight speed. The cells holding the peak value in Table 2 are (row, column) (5, 16), (4, 23) and (5, 19), which do not vary monotonically with height, in keeping with the multi-peaked longitudinal profile of Fig. 3(a). The position of a single extreme point is governed by local randomness and is unstable, so it is not used to measure the displacement of the deposit as a whole; the water-weighted centroid is used instead.

3. Discussion

3.1 Matching deposition intensity to fireline intensity

The suppression effectiveness of a bucket drop depends on how well the unit-area application amount matches fireline heat release. Byram's fireline intensity, I [15], is the fundamental descriptor of that heat-release rate. Starting from fire-point heat balance, Penney et al. [16] proposed a method for estimating the critical water application rate and showed that required water increases markedly with fireline intensity, fuel load, and fire-danger rating. Applying this method with fuel parameters representative of surface fuels in southwestern China gives a required unit-area application amount of approximately 0.5–3.0 L/m² for low-to-moderate-intensity surface fires (fireline intensity about 500–5,000 kW/m). Because this threshold is derived from engineering estimates and semi-empirical models developed mainly for fixed-wing operations—and does not account for canopy interception, fuel moisture variation, or differences between direct extinguishment and fuel wetting—it is used here only as an order-of-magnitude reference.

Set against Table 2: at 15 m the peak of 4.41 L/m² exceeds the upper end of that range and the non-zero-area mean of 0.88 L/m² still meets the requirement for low-to-moderate firelines, so this height suits direct attack on high-intensity fire. At 20 m the peak of 2.83 L/m² falls in the moderate range, the non-zero-area mean is highest (0.93 L/m²), the effective coverage area is large (1 287 m²) and the recovery ratio is highest (41.1%), giving the best combined performance. At 25 m the peak falls to 2.44 L/m² and the non-zero-area mean to 0.67 L/m², which limits effectiveness against high-intensity fire, though the coverage area is much the same as at 20 m, so this height suits weak fire, firebreak construction and mop-up. 'Best combined performance' here means the highest average wetting level over the wetted area for a loss of under 5% in effective coverage area; were uniformity of spreading the only criterion, the 25 m case would not be inferior to the 20 m one — Fig. 3(b) shows its lateral profile to be the widest and its peak the lowest — so the ranking holds only under the criteria stated. The values of w above represent 3 m × 3 m cells, whereas suppression at the scale of a fireline also requires the qualifying wetted zone to form a continuous band along it; at 3 m resolution that continuity cannot be judged, so the matching conclusions distinguish task types only and are not sufficient to derive the number of drops or the length of continuous coverage required. The ranking rests on deposition pattern and water quantities and has not been checked against ignition trials, so it is not a ranking of suppression effectiveness.

3.2 Physical mechanism behind the effect of drop height

The observations above follow from the motion of the released water. Once the valve opens, the water column accelerates downward under gravity and necks; aerodynamic forces stretch and strip it until it breaks up secondarily into a cloud of droplets. The degree of breakup is characterised by the Weber number $We = \rho_a u^2 d/\gamma$, where ρ_a is air density, u the relative air–liquid velocity, d a characteristic droplet diameter and γ the surface tension of water (σ being reserved for dispersion). During descent the droplet cloud spreads sideways under lateral aerodynamic forces and turbulent fluctuations, while droplets of different size settle at different rates: large droplets settle quickly, travel little sideways and tend to build a concentrated deposit beneath the release point, whereas small droplets stay airborne longer and spread more widely.

Drop height acts by lengthening these processes. At 15 m the fall lasts only 1.75 s; the column has not fully broken up and large masses of water reach the ground directly, giving high peak intensity, narrow lateral spread and a non-uniform pattern. At 20–25 m the fall lasts more than 2 s, the droplets get longer to break up and disperse, the size distribution shifts towards finer droplets, and the lateral distribution widens while peak intensity falls. At 25 m the fine droplets spend longer still in the air, losses to evaporation and wind drift grow [17], and the initial angular error introduced by bucket swing is amplified over the longer fall, so part of the water is thrown beyond the target area and the recovery ratio falls. The under-counting caused by the limited width of the array (Section 1.2) and the losses to evaporation and drift push in the same direction, and the present data cannot separate the two. The gains and losses of height balance near 20 m, which is why the 20 m case gives the best uniformity and the best recovery ratio together.

Release at low level adds the aerodynamic disturbance of the aircraft itself. Flying slowly 15 m above the ground, an AS350B3 produces a rotor downwash that has not fully decayed near the surface: it imposes extra lateral disturbance on the falling column and probably intensifies the secondary splash of the water on landing, which is one reason why deposition at low level is not simply ‘more concentrated’. Going lower is constrained by aircraft safety and by the clearance needed over trees and terrain, and any gain in drop accuracy becomes uncertain as the downwash disturbance strengthens, so heights below 15 m were left out of the test matrix.

Longitudinal deposit length is governed by a different mechanism. It is approximately the product of release duration and flight speed: the distance the helicopter covers while water drains continuously from the valve sets the length of the deposit. Raising the height changes the fall time but not the release duration and can therefore hardly affect longitudinal extent, which means that with a given delivery system the longitudinal extent can be adjusted only through flight speed and release timing.

3.3 Recommended drop heights for operations

In summary, the effect of drop height on deposition pattern can be characterized as higher intensity at lower altitude and greater uniformity at higher altitude, while longitudinal extent is controlled mainly by flight speed. Because the recommendations below are based on three single-drop cases and have not yet been validated by fire-behavior experiments, they should be treated as preliminary operational guidance. Practical application should also consider tree height, terrain slope, fuel conditions, wind, and fire type.

The operational recommendations are as follows:

(1) For direct attack on a high-intensity fire head or a critical fireline, use 15–18 m to obtain a peak deposition intensity above 4 L/m² and rapid cooling and knock-down. Deposition at this height is concentrated and the covered width is limited, so the drop must be lined up with the fireline and segmented drops may be needed to make up the shortfall in coverage. The height chosen must also leave the clearance that aircraft safety, tree height and terrain require.

(2) For moderate-intensity firelines, or when both suppression and wet-line construction are required, use approximately 20 m. This case provides the highest mean application over the wetted area, a recovery ratio of 41.1%, and a peak-to-mean ratio of 3.06, indicating the best balance between deposition uniformity and water-use efficiency.

(3) For building firebreaks over a large area or for mopping up, 23–25 m may be used, trading peak intensity for more even spreading. At this height the loss of fine droplets to evaporation and drift is appreciable, so a lower flight speed and a release point offset upwind of the target should be used to raise the deposit per unit area.

(4) Once the height is chosen, the forward shift should be estimated from the horizontal displacement travelled during descent and the lead distance corrected accordingly: each 10 m of height moves the

deposit about 8–10 m forward along the flight line. The measured centroid shift agrees well with the theoretical estimate and can serve as a simple rule; where the equipment allows, real-time conversion from onboard height and ground speed is preferable.

3.4 Uncertainties and further work

The conclusions are subject to the following limitations. First, each case comprised a single full-bucket drop, so the spatial randomness of the deposition pattern could not be separated by replication and differences between cases can be compared only in order of magnitude; at least three replicates per case, reported with coefficients of variation, should follow. Second, the finest resolution available is 3 m along the flight direction, set by the sampling interval, and 9 m² across it, set by the cell area, so isolated points at the edge carry disproportionate weight in parameters fixed by extremes or by counting, such as lateral deposit width and coverage area; differences below about 5% in Table 2 should not be over-interpreted. The array is only 18 m wide and the deposit at 25 m reaches that boundary, so the lateral data are right-censored; later tests should widen the array laterally or move to probabilistic measures such as the probability of achieving a given coverage level. Third, the absolute magnitude of the unit-area application amount depends on how accurately the collecting area is calibrated, and evaporative loss between release and weighing was not quantified on its own — the same operating and weighing procedure was used in every case, so this acts as a systematic bias in comparisons between cases. The recovered volume obtained directly from the weighing record and the value obtained by integrating the application-amount field over the effective coverage area do not yet close in absolute terms, which points to a systematic error still to be located in the area calibration or in the summation of the record; the bowl mouth area should be recalibrated by direct measurement, and the result checked through a closure test on the volume delivered, the drift loss and the water on the ground. Fourth, the volume actually released, the valve opening and closing sequence, the wind field over the whole descent and the droplet size spectrum were not measured, and the contribution of rotor downwash to spreading at low level cannot be isolated, so the recovery ratios in Table 2 should be read as lower bounds. Until the closure test is done, the absolute values of the peak and non-zero-area mean application amounts, and any comparison of them against water requirements for suppression, should be taken as order-of-magnitude references.

Two further points. The tests were run under light wind, with crosswind held below an upper limit rather than varied systematically, so the effect of wind speed on the drift of fine droplets remains unquantified. And because no fire-behaviour trials were conducted, the conclusions describe the deposition pattern only and do not amount to an assessment of suppression effectiveness. Later work will bring in wind speed and direction and bucket volume as variables, combine segmented release with fire-behaviour response trials, and develop a method for optimising drop parameters against the state of the fire; operating cost and the round trip for refilling will be coupled in as well, so that the characteristics of the deposition pattern can serve the assessment of suppression effectiveness directly.

4. Conclusions

(1) At a constant flight speed of approximately 70 km/h, increasing the drop height from 15 to 25 m monotonically reduces the peak areal application amount from 4.41 to 2.44 L/m², corresponding to an overall reduction of 44.7%. The reduction rate decreases with increasing height: a 35.8% reduction occurs over the 15–20 m interval, versus 13.9% over the 20–25 m interval. The deposition centroid shifts 8.5 m downstream along the flight path, and lateral dispersion increases from 0.78 to 0.95 m. Drop height primarily controls deposition intensity and lateral spreading.

(2) Longitudinal deposit length ranges from 132 to 141 m, a relative variation of only 6.4%, while the effective coverage area varies between 1260 and 1323 m², representing a reduction of 4.8%. Back-calculated release durations fall between 6.7 and 7.2 s. The longitudinal extent is determined by the product of release duration and flight speed and is therefore insensitive to drop height. The 20 m treatment yields the highest mean application over the wetted area (0.93 L/m²), the lowest peak-to-mean ratio (3.06), and the greatest water recovery fraction within the measurement array (41.1%), indicating the optimal balance between application uniformity and water-use efficiency.

(3) Within the experimental bounds reported herein, drop height may be selected provisionally according to operational objectives: 15–18 m for direct suppression of high-intensity firelines, approximately 20 m where both deposition intensity and coverage width are prioritized, and 23–25 m for constructing extensive firebreaks or conducting mop-up operations. After the drop height is selected, the lead distance should be adjusted to account for an 8–10 m downstream shift of the centroid per 10 m increase in drop height, ensuring that the water deposition overlaps the target fireline. These operational recommendations require validation via replicated bucket-drop tests and prescribed ignition trials.

Declarations

Author Contribution

Author ContributionsLI Mingxuan: Conceptualization, Methodology, Investigation, Data curation, Formal analysis, Visualization, Writing – original draft.ZHU Xiaobo: Conceptualization, Methodology, Supervision, Project administration, Funding acquisition, Writing – review & editing.LUO Wuzhou: Methodology, Resources, Validation, Writing – review & editing.All authors have read and approved the final manuscript and agree to be accountable for all aspects of the work.

Acknowledgments

This research was supported by the Science and Technology Program of the National Fire and Rescue Administration of China (Grant No. 2024XFCX24).

References

1. SHU Lifu, TIAN Xiaorui, KOU Xiaojun. The focus and progress on forest fire research (Ⅱ)[J]. World Forestry Research, 2003, 16(3): 37-40. DOI: 10.3969/j.issn.1001-4241.2003.03.008. (in Chinese)
2. WAN Xingyong, XU Jingfeng, ZHAO Fengjun, et al. Analysis on suitability of fighting mountain fire and water extraction operations in Yunnan: a case study of AS-350B3 helicopter[J]. Fire Science and Technology, 2023, 42(5): 704-708. (in Chinese)
3. WU Zepeng, ZHOU Yufei, ZHEN Xuening, et al. Effectiveness of bucket water dropping in coordinated air-ground forest fire suppression: a case study of the K-32 helicopter[J]. Forestry and Environmental Science, 2016, 32(6): 16-19. (in Chinese)
4. WU Zepeng, WU Yan, LI Su, et al. Efficiency of bucket water dropping for fire suppression: a case study of the K-32 helicopter[J]. Forest Fire Prevention, 2017(1): 34-37. (in Chinese)
5. ZHANG Wenyang, LI Qingfeng, XUE Keshun, et al. Coordinated bucket water-dropping technology for helicopter groups[J]. Forest Fire Prevention, 2023, 41(2): 72-75. (in Chinese)
6. XIE Jiayu, ZHU Yanan, RUAN Tao, et al. Experimental study on the attitude of the helicopter fire fighting bucket[J]. Fire Science and Technology, 2024, 43(7): 982-989. DOI: 10.20168/j.1009-0029.2024.07.0982.08. (in Chinese)
7. AMORIM J H. Numerical modelling of the aerial drop of firefighting agents by fixed-wing aircraft. Part I: Model development[J]. International Journal of Wildland Fire, 2011, 20(3): 384-393. DOI: 10.1071/WF09122.
8. AMORIM J H. Numerical modelling of the aerial drop of firefighting agents by fixed-wing aircraft. Part II: Model validation[J]. International Journal of Wildland Fire, 2011, 20(3): 394-406. DOI: 10.1071/WF09123.
9. SATOH K, MAEDA I, KUWAHARA K, et al. A numerical study of water dump in aerial fire fighting[C]//GOTTUK D T, LATTIMER B Y. Fire Safety Science: Proceedings of the Eighth International Symposium. Beijing: International Association for Fire Safety Science, 2005: 777-787. DOI: 10.3801/IAFSS.FSS.8-777.
10. PLUCINSKI M P, PASTOR E. Criteria and methodology for evaluating aerial wildfire suppression[J]. International Journal of Wildland Fire, 2013, 22(8): 1144-1154. DOI: 10.1071/WF13040.
11. GIMÉNEZ A, PASTOR E, ZÁRATE L, et al. Long-term forest fire retardants: a review of quality, effectiveness, application and environmental considerations[J]. International Journal of Wildland Fire, 2004, 13(1): 1-15. DOI: 10.1071/WF03001.
12. LEI Yifei, HU Jinwen, XU Zhao, et al. Modeling, optimization, and parameter calibration of aerial water dropping for multi-aircraft fire extinguishing operations[J]. Science China Technological Sciences, 2026, 69(1): 1120402. DOI: 10.1007/s11431-025-3071-5.
13. PLUCINSKI M P, MCCARTHY G J, HOLLIS J J, et al. The effect of aerial suppression on the containment time of Australian wildfires estimated by fire management personnel[J]. International Journal of Wildland Fire, 2012, 21(3): 219-229. DOI: 10.1071/WF11063.
14. WU Yingda, AN Qiuze, WU Ji, et al. Numerical simulation and analysis of water dropping from the belly-cabin of fire-fighting helicopters[J]. Fire Science and Technology, 2026, 45(2): 98-105. DOI:

10.20168/j.1009-0029.2026.02.0098.08. (in Chinese)

15. BYRAM G M. Combustion of forest fuels[M]//DAVIS K P. Forest Fire: Control and Use. New York: McGraw-Hill, 1959: 61-89.
16. PENNEY G, HABIBI D, CATTANI M, et al. Calculation of critical water flow rates for wildfire suppression[J]. Fire, 2019, 2(1): 3. DOI: 10.3390/fire2010003.
17. SUN Haoran, WU Chengyun, WANG Yanmeng, et al. Modeling and experimental study on the evaporation characteristics of liquid droplets subject to thermal convection[J]. Journal of Chemical Industry and Engineering, 2025, 76(S1): 123-132. DOI: 10.11949/0438-1157.20241404. (in Chinese)

Figures

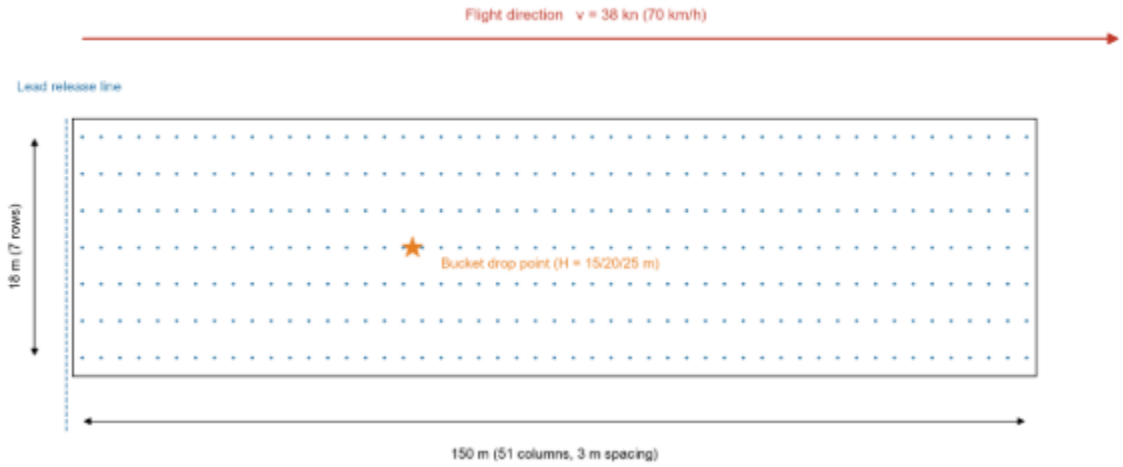


Figure 1

Arrangement of measurement points in the test area

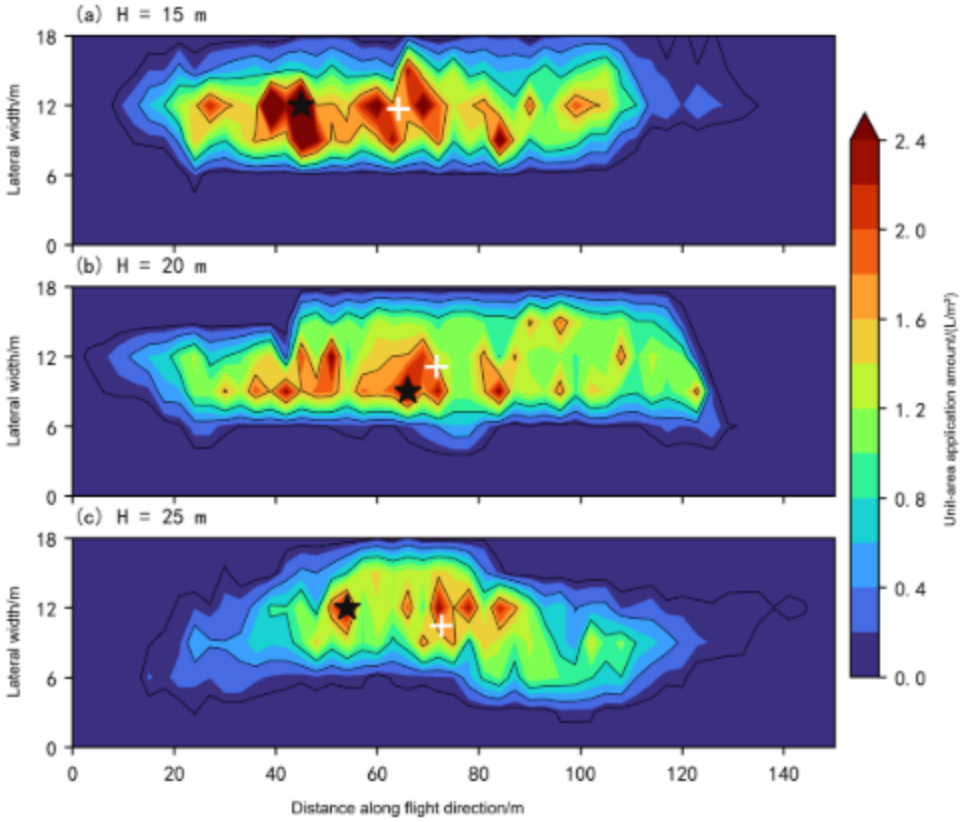


Figure 2

Contour maps of unit-area water application amount at different drop heights

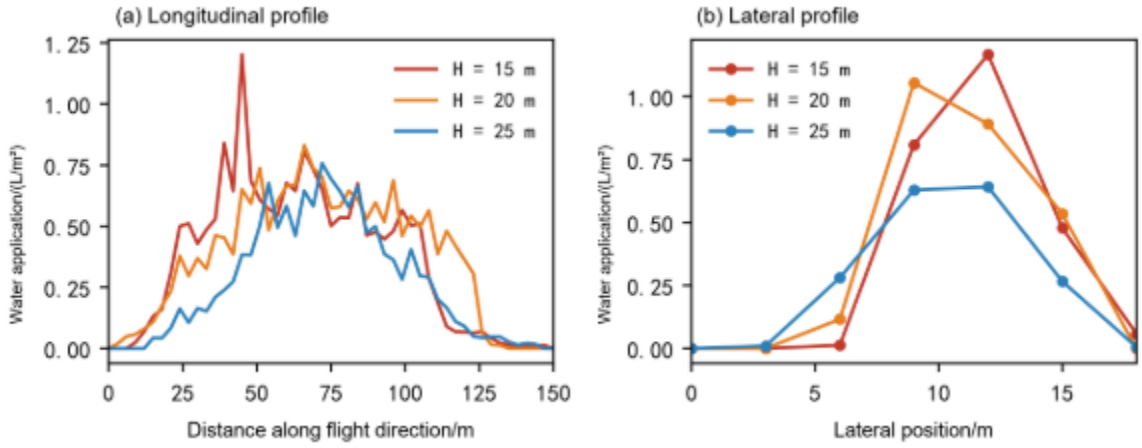


Figure 3

Deposition profiles along and across the flight direction at different drop heights

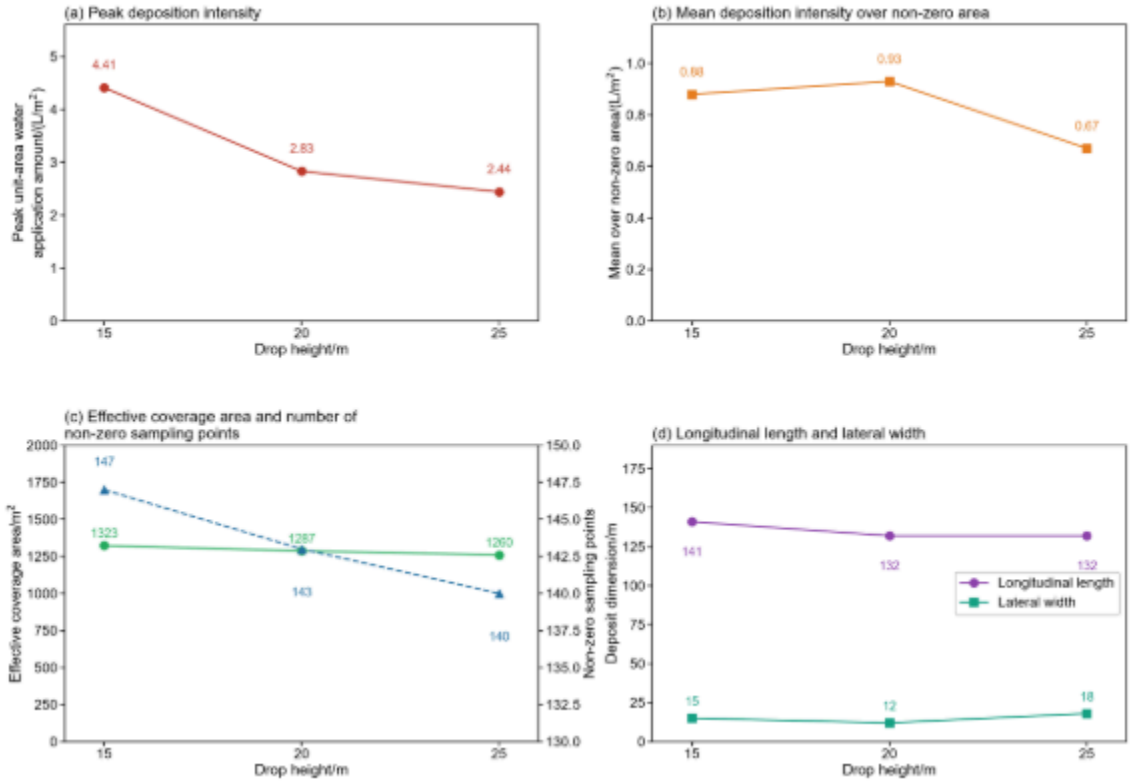


Figure 4

Variation of deposition characteristic parameters with drop height

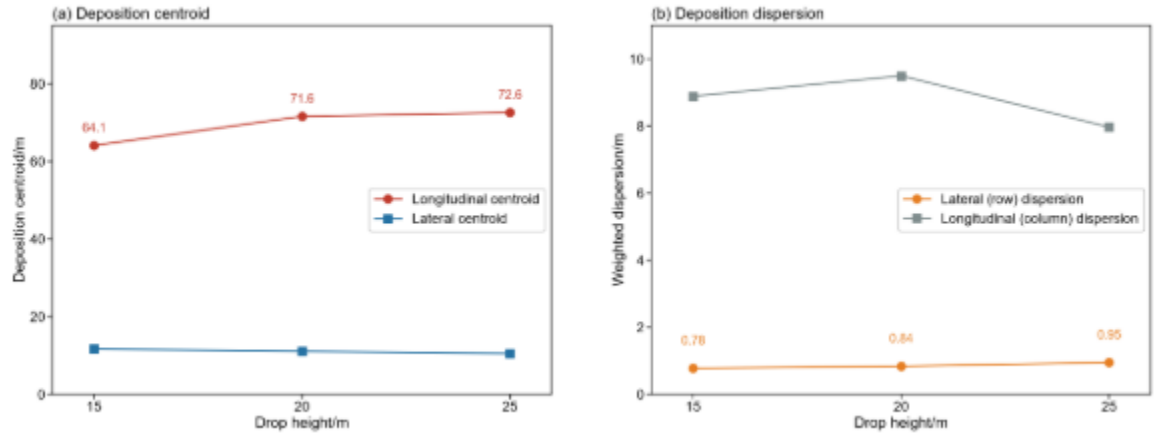


Figure 5

Variation of deposition centroid and dispersion with drop height